

# Linking outcrop analogue with flow simulation to reduce uncertainty in sub-surface carbon capture and storage: an example from the Sherwood Sandstone Group of the Wessex Basin, UK

Newell, A.J. and Shariatipour, S.M.

**Author post-print (accepted) deposited by Coventry University's Repository**

**Original citation & hyperlink:**

Newell, A.J. and Shariatipour, S.M. (2016) Linking outcrop analogue with flow simulation to reduce uncertainty in sub-surface carbon capture and storage: an example from the Sherwood Sandstone Group of the Wessex Basin, UK. *Geological Society, London, Special Publications*,, volume 436 : SP436-2

<http://dx.doi.org/10.1144/SP436.2>

DOI 10.1144/SP436.2

ISSN 0305-8719

ESSN 2041-4927

Publisher: The Geological Society

**Copyright © and Moral Rights are retained by the author(s) and/ or other copyright owners. A copy can be downloaded for personal non-commercial research or study, without prior permission or charge. This item cannot be reproduced or quoted extensively from without first obtaining permission in writing from the copyright holder(s). The content must not be changed in any way or sold commercially in any format or medium without the formal permission of the copyright holders.**

**This document is the author's post-print version, incorporating any revisions agreed during the peer-review process. Some differences between the published version and this version may remain and you are advised to consult the published version if you wish to cite from it.**

# **Linking outcrop analogue with flow simulation to reduce uncertainty in subsurface carbon capture and storage: an example from the Sherwood Sandstone Group of the Wessex Basin, UK**

**Andrew J Newell<sup>1</sup> and Seyed M Shariatipour<sup>2</sup>**

<sup>1</sup>British Geological Survey, Maclean Building, Wallingford, Oxfordshire OX10 8BB, UK

<sup>2</sup>Coventry University, Priory Street, Coventry CV1 5FB, UK

**Abstract:** Modelling the behaviour of carbon dioxide (CO<sub>2</sub>) injected into subsurface reservoirs as part of carbon capture and storage (CCS) strategies is often performed using models that incorporate very limited geological detail, particularly at the subseismic (metre to decametre) scale. Those modelling studies that incorporate varying degrees of geological realism show the inherent risks and uncertainties that can result from neglecting heterogeneity and reservoir-caprock topography along the migration path of an injected CO<sub>2</sub> plume. A key problem is that detailed geological data are often not available for the relatively deep saline aquifers that are an important target for CCS. Deep saline aquifers fall between the relatively data-rich environments of shallow freshwater aquifers and hydrocarbon reservoirs and it is in these settings that outcrop analogues may play an important part in reducing the risks and uncertainties associated with CCS. This study uses an example from the Sherwood Sandstone Group (Otter Sandstone Formation) of the Wessex Basin to show how an outcrop study can impart a much greater understanding of heterogeneity in critical reservoir-caprock zones. Here the transition from the Sherwood Sandstone Group (fluvial sandstone reservoir) to the Mercia Mudstone Group (playa lacustrine mudstone seal) is not simple, but includes a major change in fluvial style which introduces considerable heterogeneity at the top of the reservoir. The study shows how laser scanned outcrop can be used to rapidly construct static geological models which are taken through to flow simulations. In combination, the use of appropriate outcrop analogues and flow modelling can reduce the risks and uncertainties associated with CCS.

## **Keywords**

Carbon capture and storage, Sherwood Sandstone Group, outcrop analogue, flow simulation

## Introduction

Capturing carbon dioxide (CO<sub>2</sub>) from anthropogenic sources and containing it in subsurface geological formations is one option for the reduction of greenhouse gas emissions into the atmosphere (Boot-Handford et al. 2014; IPCC 2005). The world's first commercial-scale carbon capture and storage (CCS) facility is now operational at SaskPower's Boundary Dam coal-fired power plant in Estevan, Saskatchewan, Canada (Watson 2014). A variety of subsurface storage scenarios are being considered around the world including operational or depleted oil and gas reservoirs, deep saline aquifers and unmineable coal seams (Bachu et al. 2007). Secure storage of CO<sub>2</sub> is achieved through a combination of physical and chemical trapping mechanisms that are effective over different timeframes and scales (Holloway, 2009). Aside from one operational plant, CCS is still at an early stage of development with only a few large-scale field trials world-wide (Hosa et al. 2011). Moreover, none of these practical trials involves the volumes, rates and time scales which approach the anticipated requirements for CCS at an industrial scale (Nilsen et al. 2012). Model-based forecasts are therefore, critically important in understanding the risks and uncertainties associated with injecting CO<sub>2</sub> into the subsurface (Mackay 2013).

Modelling the behaviour of CO<sub>2</sub> injected into subsurface reservoirs is often performed using models that incorporate very limited geological detail, particularly at the subseismic (metre to decametre) scale (Nilsen et al. 2012). However, those modelling studies that incorporate varying degrees of geological realism show the inherent risks and uncertainties that can result from neglecting heterogeneity and reservoir-caprock topography along the migration path of an injected CO<sub>2</sub> plume (Goater et al. 2013; Lindeberg and Bergmo 2003; Nilsen et al. 2012; Shariatipour et al. 2013). A key problem is that detailed geological data are often simply not available for the relatively deep saline aquifers that are an important target for the industrial-scale sequestration of CO<sub>2</sub> (Holloway 2009). Deep saline aquifers fall between the relatively data-rich environments of shallow freshwater aquifers and hydrocarbon reservoirs and it is in these settings that outcrop analogues (Hodgetts

2013; Howell et al. 2014) may play an important part in reducing the risks and uncertainties associated with CCS.

This study uses an example from the Sherwood Sandstone Group (Otter Sandstone Formation) of the Wessex Basin to show how an outcrop study can improve our understanding of how rock heterogeneity controls the migration and trapping of buoyant CO<sub>2</sub> plumes injected into dipping saline aquifers. Here the transition from the Sherwood Sandstone Group (fluvial sandstone reservoir) to the Mercia Mudstone Group (playa lacustrine mudstone seal) is not simple, but includes a major change in fluvial style which introduces considerable heterogeneity at the top of the reservoir. The study shows how a laser scanned outcrop can be used to rapidly construct static geological models which are taken through to flow simulations. In combination, the use of carefully-selected outcrop analogues and flow modelling may reduce the risks and uncertainties associated with CCS in frontier dipping saline aquifers.

### **Mechanisms of subsurface CO<sub>2</sub> Storage**

#### *Dipping saline aquifers versus structural traps*

Conventional structural traps which generally comprise a porous reservoir rock folded or faulted into a structural high and covered by an impermeable seal are probably the most obvious way to trap buoyant CO<sub>2</sub> injected into a subsurface geological formation (Fig. 1) (Williams et al. 2013). Conventional structural traps that are operational or former hydrocarbon reservoirs are particularly attractive because of an abundance of pre-existing geological data, the potential for economic benefits from enhanced oil or gas recovery and their proven sealing capacity, subject to injected CO<sub>2</sub> not exceeding the interfacial threshold pressure for caprock breakthrough or reaching a reservoir spill point (Holloway 2009; Watson 2014). Dipping saline aquifers with no large-scale structural closure (Fig. 1) are a less obvious target for the subsurface storage of CO<sub>2</sub> although, simply because of their great abundance in sedimentary basins throughout the world, they are potentially more

important than conventional structural traps (Holloway, 2009; Ogawa et al., 2011). In dipping saline aquifers, it is envisaged that long-term storage is largely achieved through the dissolution of injected CO<sub>2</sub> into the pore fluid and the development of an irreducible 'residual' CO<sub>2</sub> saturation in pore spaces as the plume migrates through the aquifer (Holloway 2009). Counter-intuitively, although dipping aquifers are open structures, they are arguably a more secure form of storage than closed structural traps, because in the latter the risk will always remain that free CO<sub>2</sub> could escape from the reservoir if the seal is breached (Mackay 2013). However, a problem common to most dipping saline aquifers is that hard geological data from boreholes, seismic and other sources are sparse, particularly in the critical zone between the reservoir and the caprock. The morphology of this interface is one of the key areas of uncertainty in CCS modelling studies, particularly regarding the amount of structural trapping that might be anticipated and the general long-term migration of the plume (Nilsen et al. 2012; Shariatipour et al. 2013). Geological features controlling the morphology of the reservoir-seal interface are commonly only included in reservoir models if they are resolvable in seismic surveys (Nilsen et al. 2012). This is likely to exclude much of the small-scale (metre to decametre) topography and heterogeneity created by sedimentary depositional and erosional processes.

#### *The importance of the reservoir-caprock interface*

CO<sub>2</sub> is mobile and once injected it will typically migrate over large distances before becoming fully trapped. Movement is primarily driven by its greater buoyancy relative to the pore waters and once injected, generally as a supercritical fluid, it will tend to accumulate and migrate up-dip as thin layers beneath the caprock (Fig. 1). Migration will cease once all of the CO<sub>2</sub> has been structurally trapped, dissolved, left as an irreducible fraction in the pore space or chemically reacted with the host rock (Bachu et al. 2007). Until this immobile state has been achieved the morphology of the reservoir-caprock interface can have an important influence on the migration of the plume. Modelling studies have shown that minor structural and stratigraphic traps ('bumps') and sedimentary heterogeneity

along the migration path of the CO<sub>2</sub> can have a significant effect on the amount of physical trapping and the general form and migration distance of the plume (Bachu et al. 2007; Goater et al. 2013; Pickup et al. 2011; Shariatipour et al. 2013).

### *The importance of the Sherwood Sandstone Group to UK CCS*

In southern Britain, Triassic rocks are predominantly terrestrial deposits that accumulated within a series of linked rift basins which connected southern sediment sources in the Variscan fold-belt with major sediment sinks in the East Irish Sea and Southern North Sea basins to the north (McKie and Williams 2009; Morton et al. 2013) (Fig. 2). Excellent storage prospects for CO<sub>2</sub> within the Triassic basin-fill are created by an upward transition in the Triassic stratigraphy from the reservoir sands of the Sherwood Sandstone Group (and Bunter Formation) at the base, into sealing mudstones and evaporites of the Mercia Mudstone (and Haisborough) groups (Fig. 3). The Triassic Sherwood Sandstone Group, and broadly correlative units such as the Bunter Formation in the Southern North Sea (Williams et al. 2013), are some of the key formations being considered for CO<sub>2</sub> storage in the UK (Armitage et al. 2013). The switch from reservoir sandstone to sealing mudstone is complex, both in terms of its temporal distribution and in the sedimentological architecture of the transition interval. Biostratigraphy and magnetostratigraphy show that the Sherwood Sandstone Group-Mercia Mudstone Group boundary is strongly diachronous, becoming younger southwards as coarse-grained fluvial systems retreated toward their sources in the Variscan mountain belt (Hounslow and McIntosh 2003).

Throughout much of the subsurface, particularly in areas of saline aquifers, data on the Sherwood Sandstone Group are sparse and here outcrop analogues may have a considerable significance in terms of gaining greater understanding of sub-seismic heterogeneity and reservoir-caprock morphology. In this paper we examine some large-scale outcrop of the Triassic Sherwood Sandstone Group (Otter Sandstone Formation) in the western part of the Wessex Basin in south Devon, England (Fig. 2). The paper aims to show how outcrop can improve our understanding of sedimentary

heterogeneity at reservoir-caprock interfaces beyond what might be achieved by using sparse subsurface datasets alone. It also aims to demonstrate how modern field tools such as terrestrial laser scanners make it a relatively straightforward task to extend field studies into dynamic flow simulations which may increase the value of the outcrop work still further.

### **The Sherwood Sandstone Group of the Wessex Basin**

The Triassic Sherwood Sandstone Group crops out along the western margin of the Wessex Basin, an area of extensional faulting in southern England that was episodically-active between the Permian and Cretaceous periods (Newell 2000) (Fig. 4). The broadly north-south orientated outcrop of the Sherwood Sandstone Group intersects the northwest-southeast trending coastline between Budleigh Salterton and Sidmouth in south Devon where virtually the entire succession can be seen in spectacular sea-cliff exposures (Fig. 5). The Sherwood Sandstone Group comprises the conglomeratic Budleigh Salterton Pebbles Beds (around 30 m thick) overlain by the Otter Sandstone Formation which is around 200 m thick. Approximately 8 m of aeolian sandstone occur at the base of the Otter Sandstone Formation (Wright et al. 1991), but the bulk of the formation is composed of vertically and laterally amalgamated fluvial sheet sandstones (Newell 2006). Mudstone mostly occurs as occasional isolated channel plugs, apart from the uppermost 15 m of the Otter Sandstone Formation, where it increases greatly in abundance in a subdivision called the Pennington Point Member, immediately beneath the Sidmouth Mudstone Formation, the lowermost unit of the Mercia Mudstone Group (Gallois 2005). From its western outcrop, the Otter Sandstone Formation dips below the thick Jurassic and Cretaceous fill of the Wessex Basin and it forms an important hydrocarbon reservoir at Wytch Farm (Bowman et al. 1993). Boreholes provide evidence for some fault-control on the facies and thickness patterns of the Otter Sandstone Formation, particularly toward the base of the formation where thick intervals of anhydritic mudstone are locally present (Fig. 4) (Holloway et al. 1989).

The primary focus of this study is on the uppermost part of the Otter Sandstone Formation (Pennington Point Member) because in a carbon capture and storage scenario this region would form the reservoir-caprock interface under which buoyant CO<sub>2</sub> would accumulate and spread. In south Devon this part of the stratigraphy is superbly exposed under High Peak to the west of Sidmouth where it occurs at an elevation of around 30 m above sea level (Fig. 5). By a combination of a northeasterly structural dip and several down-to-the-east faults the Pennington Point Member reaches sea-level at Tortoiseshell Rocks on Sidmouth beach (Fig. 4). Faulting repeats the unit at Pennington Point, immediately east of Sidmouth (Gallois 2005).

### **The Pennington Point Member at the reservoir-caprock interface**

The Pennington Point Member is around 15-20 m thick and has an erosive contact with the underlying amalgamated sheet sandstones (Chiselbury Bay Member) of the Otter Sandstone Formation (Fig. 6). Localised scours on this basal erosion surface are variably infilled with sandstone, mudstone or a combination of both (Fig. 6). The upper contact of the Pennington Point Member with the massive reddish-brown mudstones of the Mercia Mudstone Group is gradational, often with a progressive decrease in sandstone bed thickness (Fig. 7). Sandstone and mudstone occurs in approximately equal proportions in the Pennington Point Member, although there is lateral variation due to the thickening and thinning of the beds. The sandstones are weakly cemented, often micaceous, very fine- to fine-grained and moderately sorted. A number of distinct lithofacies can be recognised within the Pennington Point Member which are summarised below.

#### *Amalgamated channel-bar and channel-plug complexes*

These sandstone-dominated units range up to 3 m thick and have a sheet-like geometry. The base of each sheet is an erosion surface, often marked by an abundance of mudstone rip-up clasts. The internal structure of sheets is complex and most are built from laterally and vertically amalgamated sandstone bodies up to 1 m thick which are separated by erosion surfaces and thin mudstone drapes

(Fig. 6). Individual sandstone bodies tend to have flat bases and concave-down tops. Where internal structure is discernible, the sandstone bodies are predominantly trough cross-bedded, although tabular cross-bedding and ripple cross-lamination can also occur. Traced laterally, individual sandstone bodies commonly wedge out into metre-thick mudstone plugs with flat tops and concave-up bases.

These complex sheet-like deposits probably represent an amalgamation of fluvial channel-bar and channel-plug deposits (Bridge 2003). An abundance of internal erosion surfaces indicates multiple episodes of channel migration and avulsion within a broad channel belt. Mudstone plugs represent the fill of former channels.

#### *Isolated point-bar deposits*

Isolated point bar deposits are best observed in the cliffs at High Peak near Big Picket Rock (Fig. 5) where they occur immediately below the Mercia Mudstone Group. This part of the cliff cannot be accessed directly but a terrestrial laser scanner with an integrated digital camera (Hodgetts 2013) was used to create a virtual digital outcrop model and an undistorted base-map (Fig. 5). The point bar deposits are up to 6 m thick and comprise a lower bar core composed of trough cross-bedded sandstone which pass upwards and laterally into a series of inclined sandstone and mudstone bed couplets which downlap onto a relatively horizontal basal erosion surface.

These deposits represent the relatively complete preservation of a fluvial point bar. Trough cross-bedded sandstone represents lower point bar deposits deposited close to the channel floor by sinuous-crested dunes while the overlying and off-lapping inclined sandstone-mudstone couplets represent lateral accretion of the bar-top (Bridge 2003). These remarkably preserved point bar deposits probably owe their preservation to the relatively passive drowning associated with the transgression of the overlying Mercia Mudstone Group. The undulating contact between the Otter Sandstone Formation and Mercia Mudstone Group is effectively a drowning unconformity.

### *Splay sandstones*

These are represented by intervals of relatively thin (< 1 m) tabular or lenticular sandstone beds interbedded with mudstone. Sandstone beds generally have erosive bases, often with distinct gutters along their base, and a discontinuous lenticular geometry (Fig. 5). Sandstone beds are commonly massive, but can show small-scale trough cross-bedding or ripple cross-lamination. Mudstone beds are massive, dark reddish brown and lenticular with occasional discontinuous sand laminae and sand-filled desiccation cracks, burrows and water escape structures (Fig. 8).

These thin sandstone beds probably represent small-scale overland flood events that were unconfined or only weakly confined within shallow channels. Interbedded mudstones were probably deposited from suspension following each flood event. Given the evidence for the co-existence of large river channels, flood events could have been initiated from lateral overbank flood events which would have built up levees adjacent to the main river channel, or from frontal splays downstream from a distributary channel (McKie and Williams 2009).

### *Floodbasin muds*

Floodbasin mudstones are dominated by reddish brown mudstones in laterally-extensive beds, which are typically up to 1 m thick. The mudstones generally appear massive, but include sandstone as thin lenses and laminae, within fluid escape structures and as the fill to subvertical cylindrical burrows up to 10 mm in diameter (Fig. 8). These muds were deposited from suspension on floodplains and in temporary lakes. The lack of palaeosols suggests relatively continuous sedimentation.

Taken together, the sedimentary lithofacies points toward a meandering fluvial environment for the Pennington Point Member of the Otter Sandstone Formation with sandy channel belt deposits passing laterally (and probably also in a downstream direction) into thinly-bedded splay sandstones and muddy flood-basin deposits. Relative to the amalgamated braided fluvial sheet sandstones of

the underlying Otter Sandstone Formation (Chiselbury Bay Member), this interval of muddy meandering fluvial deposits is heterogeneous and introduces considerable complexity into the reservoir-caprock transition zone. In particular, a profusion of inclined or concave-down sandstone beds terminating up dip against mudstone drapes or more laterally-extensive floodplain deposits (Fig. 5) have the potential to form stratigraphic traps for buoyant CO<sub>2</sub>. Numerous mudstone baffles and complex connectivity between sandstone bodies created by basal scour, sand-filled water escape structures and burrows (Fig. 8) is likely to create a tortuous flow path.

### **Building a static geological model**

#### *Base maps from laser scanning*

Laser scanning geological exposures using ground-based instruments is now a routine technique in field geology where direct access is difficult or dangerous or where an accurate base-map is required for the mapping and measurement of geological structures (Hodgetts 2013; Howell et al. 2014). Laser scanning generates a dense cloud of points, each with a Cartesian coordinate, which together replicate the topography of the geological exposure with millimetre accuracy. Points can be migrated into real world coordinates by establishing the location of the laser scanner using differential Global Positioning System (dGPS). Moreover, by mounting a digital camera on the laser scanner each point can be painted with Red, Green, Blue (RGB) intensity to produce a photo-realistic digital outcrop model (Hodgetts 2013). Laser scanned cliff sections were the starting point for the construction of static and dynamic flow models in this study (Fig. 9).

Three laser scans of the Otter Sandstone Formation-Mercia Mudstone Group transition were obtained at Big Picket Rock, Tortoiseshell Rocks and Pennington Point (Fig. 4). The process of converting laser scans into static geological models is illustrated using data from Peak Hill (Fig. 5). Here laser scanning was the only option to obtain scaled information on the shape and dimensions of sedimentary deposits which were otherwise inaccessible. This section was also important

because, unlike the more accessible exposures, it offered a cross-section of the deposits that was cut at a high-angle to the regional (north to northeast) palaeoflow direction. Laser scanning using Riegl LPM2K equipment was undertaken at low tide to maximise the distance between the laser scanner and the target cliff. Tides are clearly an important consideration when undertaking laser scanning on intertidal marine platforms as the process is relatively slow. The dense point clouds generated by the scanner was migrated into real world (British National Grid) coordinates and each point was attributed with an RGB value using digital photographs from the scanner-mounted camera. The point clouds were edited to remove unwanted points before meshing into a continuous triangulated irregular network (TIN). RGB values were transferred as a property onto the mesh and interpolated to improve the rendering of virtual cliff face. The digital outcrop model was used as a base map for mapping sedimentological features such as sandstone and mudstone beds (Fig. 5).

#### *Extrapolating mapped structures into 3D*

It is very usual that the full 3D geometry of a sedimentary deposit can be determined, even in areas of exceptional exposure where erosion provides multiple cross-sections in different orientations. An understanding of the full 3D geometry of a sedimentary deposit generally requires careful sequential excavation, although geophysical techniques such as ground-penetrating radar provide a useful and non-destructive alternative (Kostic and Aigner 2007). In the absence of hard physical data, qualitative or quantitative sedimentary process models can assist greatly in the extension of mapped 2D sections and 1D boreholes into an unknown rock volume (Willis and Tang 2010). The approach taken in this study was simply to extrude the mapped sedimentary facies boundaries (Fig. 5) perpendicular to the cliff section (Fig. 9A). This approach was not only rapid and technically simple, but considered reasonable in this case given, (1) the relatively small volume of the cube, (2) supporting observations on the geometry and lengths of bedding units in flow parallel and flow transverse section and (3) a desire to maintain the integrity of mapped observations rather than introduce assumptions on bed length, geometry and the overall 3D form of the deposit. This

approach is clearly not applicable to all situations, particularly where the geological model is much larger than the typical dimensions of beds or discrete sedimentary building blocks. Here the modelled volume had dimensions of 50 m x 35 m x 30 m and was discretised into 100 x 70 x 150 regular cells (Fig. 9A). The grid was subdivided into three main regions, a lower region representing the amalgamated sheet sandstones (Chiselbury Bay Member) of the Otter Sandstone Formation, a middle region representing the heterogeneous mudstone and sandstone of the Pennington Point Member and an upper region representing the Mercia Mudstone Group. The position of horizontal and inclined mudstone baffles was incorporated within the Pennington Point Member together with the undulating topography created by the point-bar deposits beneath the drowning unconformity at the base of the Mercia Mudstone Group (Fig. 5). The structural tilt of the formations was 6° toward the southeast.

#### *Porosity and permeability values*

Porosity and permeability values for the sandstone were based on core plugs taken from outcrop and neighbouring borehole core of the Otter Sandstone Formation (Allen et al. 1997; Newell 2006) (Fig. 10). Porosity values range from approximately 5 to 35% and permeability from 0.001 to 10000 millidarcys (mD). In the model, the relatively coarser-grained braided fluvial sheet sandstones of the Chiselbury Bay Member of the Otter Sandstone Formation were given a fixed porosity value of 30% while the finer-grained sandstones of the Pennington Point Member were assigned a range of porosity values using sequential Gaussian simulation (SGS) based on a normal distribution with mean of 20% and a standard deviation of 2%. The correlation between porosity and horizontal permeability was derived from core plug data (Fig. 10). Vertical permeability was set at 80% of the horizontal permeability based on the typical variation between horizontal and vertical core plug measurements (Allen et al. 1997). Mudstone was assigned constant values of 10% porosity, a typical value for the Mercia Mudstone Group (Armitage et al. 2013) and a constant permeability of 0.02 mD. This permeability is considerably higher than direct measurements from core of the Mercia

Mudstone Group, where values can be as low as 10 nanodarcys (nD) (Armitage et al. 2015). A value higher than those measured from core plugs was selected to account for the presence of sand-filled burrows (Fig. 8A), sand-filled fluid injection structures (Fig. 8B) and sandy laminae within the lowermost part of the Mercia Mudstone Group in south Devon. However, it would clearly be of interest to undertake additional modelling runs where the permeability contrast between the sandstones and mudstones was progressively increased to reflect the measured Mercia Mudstone Group values of Armitage et al. (2015). Disparities in the permeability of the Mercia Mudstone Group determined from direct measurement of core and field-derived hydraulic conductivity values, which are generally much higher (Armitage et al. 2015), show the desirability of using a quantitative approach (e.g. Pickup & Hern 2002) to estimate the effective permeability of representative volumes of reservoir and caprock. It is also appreciated that the generalised outcrop and shallow aquifer porosity and permeability values selected for this model will not necessarily be representative of the Otter Sandstone Formation at greater depths where calcite, dolomite and anhydrite may occlude some or all of the porosity within the sandstones (Holloway et al. 1989). However, it might be anticipated that, where porosity is not entirely occluded by pore-filling cement, the contrast in the porosity and permeability of the sandstone and mudstone beds, which is the primary aspect being explored in this modelling study, will still be valid.

### **Dynamic model setup**

The grid for the dynamic flow model had dimensions of 50 m × 35 m × 30 m and was discretized into 100 × 70 × 150 cells. One injector was placed on the down-dip (eastern) side of the model and CO<sub>2</sub> was injected through perforations at the bottom of the aquifer (bottom 25 layers) (Fig. 9B). The model was taken down to 1 km depth and the pore volume of the outer column of cells on the left and right hand side of the model were multiplied by a factor of 1000 to take account of this.

The well was controlled by the surface rate with a maximum pressure limit of 190 bars. CO<sub>2</sub> was injected during 6 years (around 3 million tonnes of CO<sub>2</sub> in total), and after that the model was run for 100 years to study the CO<sub>2</sub> plume migration. Initial pressure and initial temperature were set to 100 bars and 45°C at 1000 m depth. Initially, it was assumed that the reservoir contained 100% brine, with mole fraction of 0.967 and 0.033 for water (H<sub>2</sub>O) and sodium chloride (NaCl), respectively. The simulations were performed using ECLIPSE 300 compositional simulator with the CO2STORE option (Schlumberger 2013). Re-Studio and Petrel were used for pre and post-processing respectively.

### **Dynamic modelling results**

In the most geological storage cases being considered, CO<sub>2</sub> is injected in a supercritical (sc) state, which is above 31.1°C and 73.9 bars. Supercritical CO<sub>2</sub> is a fluid with a liquid-like density and a gas-like viscosity, which generally occurs at a depth of storage of more than 800 metres. In this study, CO<sub>2sc</sub> is also injected into the saline aquifer model and will stay supercritical because the minimum pressure and temperature in the model are above the least pressure and temperature for the supercritical CO<sub>2</sub> conditions.

When CO<sub>2</sub> is injected into saline aquifers, it is retained through four basic trapping mechanisms: structural/stratigraphic, dissolution, residual trapping and migration trapping (Holloway 2009). Structural/stratigraphic trapping is the most significant trapping mechanism in the short term (IPCC 2005) before the CO<sub>2</sub> dissolves in the pore fluids and reacts with mineral components of the rock. Our short-duration model runs were primarily concerned with short-term structural/stratigraphic trapping.

The density of free phase CO<sub>2</sub> is much lower than formation brine. Therefore, when free CO<sub>2</sub> is injected into the model, it migrates upwards under buoyancy until it reaches low permeability layers and then spreads out laterally (Fig. 11). This lateral migration depends on the extension of the low permeability layers and also the capillary entry pressure. Because of the discontinuity of these

mudstone baffles in the modelled volume (Fig. 9A) and also the relatively high permeability (0.02mD) assigned to them, a proportion of the injected CO<sub>2</sub> approaches, but does not reach the main reservoir-caprock interface at the base of the Mercia Mudstone Group (Fig. 11). The simulation results clearly show that the existence of multiple mudstone baffles in the upper part of the Otter Sandstone Formation aquifer enhances security of CO<sub>2</sub> storage by preventing vertical migration of CO<sub>2</sub> towards the main caprock. Subsequently, more CO<sub>2</sub> migrates laterally and more CO<sub>2</sub> dissolves in fresh brine. As CO<sub>2</sub> saturated brine is denser than pure brine, it therefore, sinks into the main storage formation represented by the more homogeneous braided sheet sandstones of the Otter Sandstone Formation (Fig. 11), and this can also initiate the convective mixing process (Lindeberg and Bergmo 2003), which could accelerate CO<sub>2</sub> dissolution in brine. The large-scale point-bar deposits which are seen immediately beneath the Mercia Mudstone Group are likely to form particularly effective stratigraphic traps for CO<sub>2</sub> because of their inclined to concave-down geometry (Fig. 5). The modelling shows that they can cause a reversal in the migration direction of the CO<sub>2</sub> plume where the stratal dip of the inclined heterolithic stratification is counter to that of the regional structural dip (Fig. 11).

In order to investigate the effect of grid size effect, the base case model modified by coarsening the model in X, Y and Z by a factor of 2, 2 and 5, respectively. Although coarsening the model reduces the simulation run time significantly due to the decrease in the number of cells from 1,050,000 cells to 52,500 cells. However, the accuracy of flow simulation of CO<sub>2</sub> storage drops due to two factors. Firstly, it diminishes the effect of small scale heterogeneities in the model. Secondly, it increases the numerical dispersion errors (Shariatipour 2013) thus increases the amount of CO<sub>2</sub> dissolution in the model and shrinks plume migration (Figs 12A, 12B).

Farhat et al., (2015) investigated the effect of capillary pressure on plume migration and CO<sub>2</sub> dissolution using the same model. In this study, the permeability range used for the Sherwood Sandstone and Mercia Mudstone groups was modified and different capillary pressure curves were

also used. Results showed that using different capillary pressure curves for different regions (permeability variation) has an effect on the plume migration and CO<sub>2</sub> dissolution (Fig. 12C). That means using more accurate data or small scale characterization of the storage formation, especially just beneath the caprock, is very important for CO<sub>2</sub> storage.

## **Discussion**

Outcrop work provides information at a resolution that lies between borehole core and seismic data (Howell et al. 2014) and may be particularly important for CCS prospects in saline aquifers where existing subsurface geological data are sparse and new subsurface data are extremely expensive to acquire.

Great care must clearly be taken to match each subsurface situation with an appropriate outcrop analogue. Even within the same region or basin there may be great variability at a particular lithostratigraphic level. This is readily illustrated by the diachronous and sedimentologically variable contact between the Sherwood Sandstone and Mercia Mudstone groups (McKie and Williams 2009). In the Wessex Basin (as discussed here) the contact between the Sherwood Sandstone Group and the Mercia Mudstone Group is marked by a shift from amalgamated 'braided' channel sandstones toward muddy meandering channel and floodplain deposits. However, in the East Irish Sea Basin the Mercia Mudstone Group transgression was preceded by the development of aeolian sand sheet and sabkha deposits of the Omskirk Sandstone Formation (Herries and Cowan 1997). Further south in the Cheshire Basin, trace fossils provide evidence for the development of intertidal sand and mud flats in the Tarporley Siltstone Formation at the base of the Mercia Mudstone Group (Pollard 1981). Elsewhere back-stepping fluvial systems at the top of the Sherwood Sandstone Group appear to have simply dispersed their water and sandy sediment load as thin diffuse sheets across low-gradient mudflats (McKie and Williams 2009). A minimum of subsurface data is clearly required to

match the reservoir with the potential outcrop analogue. The correct analogue may not come from the same time-frame or sedimentary basin as the reservoir under consideration.

Despite the operational status of the world's first commercial-scale CCS facility in Canada (Watson 2014), subsurface carbon storage is still at an early stage of development with relatively few large-scale field trials: modelling studies are still at the forefront of understanding the risks and uncertainty associated with injecting CO<sub>2</sub> into the subsurface (Mackay 2013). Most modelling studies operate on coarse (decametre) grids and over large (kilometre) areas but the importance of a multi-scalar approach has been highlighted by some workers (Nilsen et al. 2012). Modern fieldwork methods such as terrestrial laser scanning now make it a relatively straightforward process to build digital outcrop models in a form suitable for undertaking flow simulation, although challenges still remain with extrapolating hard data from outcrops into a 3D volume (Willis and Tang 2010). However, even with such limitations, flow models based on outcrop are useful for understanding how small-scale geological heterogeneity influences the movement of CO<sub>2</sub>. This study clearly shows how the addition of localised stratigraphic traps and closures below the main reservoir-caprock interface causes the immobilisation of high saturation CO<sub>2</sub>. This has been shown to be an important factor in increasing storage efficiency because it prevents the CO<sub>2</sub> plume rising and spreading along the top of the reservoir, thus bypassing much of the available pore volume (Ambrose et al. 2008; Lindeberg and Bergmo 2003). Moreover, mudstone baffles improve the lateral sweep of CO<sub>2</sub> after injection, leading to greater reservoir contact and lower migration velocities (Goater et al. 2013). This would be expected to lead to more residual trapping and dissolution (Juanes et al. 2006; Lengler et al. 2010).

Although methods such as laser scanning greatly increase the accuracy of facies mapping from large inaccessible cliff sections there are still many uncertainties in the input parameters (e.g. mudstone shape and dimension, porosity and permeability) for both the static geological modelling and the dynamic flow modelling. The results presented in this study illustrate a single realisation of the static

geological model and a limited number of flow simulations. It would clearly be desirable to extend this work toward multiple model realisations so that the sensitivity of the results to porosity, permeability, mudstone length and other variables can be fully understood before they are applied to real-world situations.

Possibly of equal importance to increased technical understanding is that outcrop studies, when carried through to flow simulations, serve as a means of promoting dialogue between geologists and flow modellers. They provide a very tangible sense of how much geological heterogeneity might be contained within a single cell of a simulation grid.

## **Conclusions**

- Facies mapping of laser-scanned cliff faces in southwest England shows that the contact between the Sherwood Sandstone (Otter Sandstone Formation) and Mercia Mudstone Group (Sidmouth Mudstone Formation) is not a simple planar surface but a complex transition through heterogeneous point-bar sandstones and sheet-like splay deposits.
- With some understanding of the porosity and permeability of the constituent facies it is possible to convert facies maps derived from laser-scanned cliff faces into attributed digital outcrop models for the purposes of flow simulation.
- Flow simulation shows that the arrangement of inclined point-bar sandstones, horizontal splay sandstones and mudstone baffles in the upper part of the Sherwood Sandstone Group produces complex flow paths with much greater potential for dispersed physical trapping of buoyant fluids such as injected CO<sub>2</sub>. Flow simulations based on the assumption of a simple, inclined planar interface between reservoir and caprock are liable to be incorrect.
- Combining outcrop analogue with flow simulation provides a cost-effective means of providing additional insight into what might control the morphology and magnitude of injected CO<sub>2</sub> plumes in the subsurface. Care must be taken that the outcrop is appropriately matched to the subsurface geology.

## Acknowledgements

S M Shariatipour thanks Schlumberger for the use of Eclipse 300 and Petrel and Amarile for the use of the Re-Studio. Marcus Dobbs and David Morgan (BGS) are thanked for their hard work and expertise with the terrestrial laser scanner. Antoni Milodowski, Richard Worden and Simon Passey are thanked for their constructive comments and editorial work on the manuscript. A J Newell publishes with permission of the Executive Director of the British Geological Survey.

## References

- Allen, D.J., Brewerton, L.J., Coleby, L.M., Gibbs, B.R., MacDonald, A.M. & Williams, A.T. 1997. The physical properties of major aquifers in England and Wales. British Geological Survey. British Geological Survey, 333pp. WD/397/034.
- Ambrose, W.A., Lakshminarasimhan, S., Holtz, M.H., Núñez-López, V., Hovorka, S.D. & Duncan, I. 2008. Geologic factors controlling CO<sub>2</sub> storage capacity and permanence: case studies based on experience with heterogeneity in oil and gas reservoirs applied to CO<sub>2</sub> storage. *Environmental Geology*, **54**, 1619-1633.
- Armitage, P.J., Worden, R.H., Faulkner, D.R., Aplin, A.C., Butcher, A.R. & Espie, A.A. 2013. Mercia Mudstone Formation caprock to carbon capture and storage sites: petrology and petrophysical characteristics. *Journal of the Geological Society*, **170**, 119-132.
- Armitage, P.J., Worden, R.H., Faulkner, D.R., Butcher, A.R. and Espie, A.A., 2015. Permeability of the Mercia Mudstone: suitability as caprock to carbon capture and storage sites. *Geofluids*, Accepted manuscript online: 25 Feb. 2015, DOI: 10.1111/gfl.12134.
- Bachu, S., Bonijoly, D., Bradshaw, J., Burruss, R., Holloway, S., Christensen, N.P. & Mathiassen, O.M. 2007. CO<sub>2</sub> storage capacity estimation: Methodology and gaps. *International Journal of Greenhouse Gas Control*, **1**, 430-443.
- Boot-Handford, M.E., Abanades, J.C., Anthony, E.J., Blunt, M.J., Brandani, S., Mac Dowell, N., Fernandez, J.R., Ferrari, M.-C., Gross, R., Hallett, J.P., Haszeldine, R.S., Heptonstall, P., Lyngfelt, A., Makuch, Z., Mangano, E., Porter, R.T.J., Pourkashanian, M., Rochelle, G.T., Shah, N., Yao, J.G. & Fennell, P.S. 2014. Carbon capture and storage update. *Energy & Environmental Science*, **7**, 130-189.
- Bowman, M.B.J., McClure, N.M. & Wilkinson, D.W. 1993. Wytch Farm oilfield: deterministic reservoir description of the Triassic Sherwood Sandstone. *Geological Society, London, Petroleum Geology Conference series*, **4**, 1513-1517.
- Bridge, J.S. 2003. Rivers and floodplains: forms, processes, and sedimentary record. Blackwell Science, Oxford.

- Farhat, M. M., Shariatipour, S. M. & Andrew, J. N. 2015. The Effect of Capillary Pressure on the CO<sub>2</sub> Storage at the Interface between Caprock and Storage Formation. *3rd International Symposium on Energy Challenges & Mechanics, Aberdeen, Scotland*.
- Gallois, R.W. 2005. The type section of the junction of the Otter Sandstone Formation and the Mercia Mudstone Group (mid Triassic) at Pennington Point, Sidmouth. *Geoscience in south-west England - Proceedings of the Ussher Society*, **11**, 51-58.
- Goater, A.L., Bijeljic, B. & Blunt, M.J. 2013. Dipping open aquifers—The effect of top-surface topography and heterogeneity on CO<sub>2</sub> storage efficiency. *International Journal of Greenhouse Gas Control*, **17**, 318-331.
- Herries, R.D. & Cowan, G. 1997. Challenging the 'sheetflood' myth: the role of water-table-controlled sabkha deposits in redefining the depositional model for the Ormskirk Sandstone Formation (Lower Triassic), East Irish Sea Basin. *Geological Society, London, Special Publications*, **124**, 253-276.
- Hodgetts, D. 2013. Laser scanning and digital outcrop geology in the petroleum industry: A review. *Marine and Petroleum Geology*, **46**, 335-354.
- Holloway, S. 2009. Storage capacity and containment issues for carbon dioxide capture and geological storage on the UK continental shelf. *Proceedings of the Institution of Mechanical Engineers, Part A: Journal of Power and Energy*, **223**, 239-248.
- Holloway, S., Milodowski, A.E., Strong, G.E. & Warrington, G. 1989. The Sherwood Sandstone Group (Triassic) of the Wessex Basin, southern England. *Proceedings of the Geologists' Association*, **100**, 383-394.
- Hosa, A., Esentia, M., Stewart, J. & Haszeldine, S. 2011. Injection of CO<sub>2</sub> into saline formations: Benchmarking worldwide projects. *Chemical Engineering Research and Design*, **89**, 1855-1864.
- Hounslow, M.W. & McIntosh, G. 2003. Magnetostratigraphy of the Sherwood Sandstone Group (Lower and Middle Triassic), south Devon, UK: detailed correlation of the marine and non-marine Anisian. *Palaeogeography, Palaeoclimatology, Palaeoecology*, **193**, 325-348.
- Howell, J.A., Martinius, A.W. & Good, T.R. 2014. The application of outcrop analogues in geological modelling: a review, present status and future outlook. *Geological Society, London, Special Publications*, **387**, 1-25.
- IPCC. 2005. Intergovernmental Panel on Climate Change, Special Report, Carbon Dioxide Capture and Storage, Summary for Policymakers, Montreal, Canada.
- Juanes, R., Spiteri, E.J., Orr, F.M. & Blunt, M.J. 2006. Impact of relative permeability hysteresis on geological CO<sub>2</sub> storage. *Water Resources Research*, **42**, W12418.
- Kostic, B. & Aigner, T. 2007. Sedimentary architecture and 3D ground-penetrating radar analysis of gravelly meandering river deposits (Neckar Valley, SW Germany). *Sedimentology*, **54**, 789-808.
- Lengler, U., De Lucia, M. & Kühn, M. 2010. The impact of heterogeneity on the distribution of CO<sub>2</sub>: Numerical simulation of CO<sub>2</sub> storage at Ketzin. *International Journal of Greenhouse Gas Control*, **4**, 1016-1025.

- Lindeberg, E. & Bergmo, P. 2003. The long-term fate of CO<sub>2</sub> injected into an aquifer. *Greenhouse Gas Control Technologies*, **1**, 489-494.
- Mackay, E.J. 2013. Modelling the injectivity, migration and trapping of CO<sub>2</sub> in carbon capture and storage (CCS). In: Gluyas, J. & Mathias, S. (eds.) *Geological storage of carbon dioxide (CO<sub>2</sub>)*. Woodhead Publishing, Cambridge, 45-70.
- McKie, T. & Williams, B. 2009. Triassic palaeogeography and fluvial dispersal across the northwest European Basins. *Geological Journal*, **44**, 711-741.
- Morton, A., Hounslow, M.W. & Frei, D. 2013. Heavy-mineral, mineral-chemical and zircon-age constraints on the provenance of Triassic sandstones from the Devon coast, southern Britain. *Geologos*, **19**, 67-85.
- Newell, A.J. 2000. Fault activity and sedimentation in a marine rift basin (Upper Jurassic, Wessex Basin, UK). *Journal of the Geological Society*, **157**, 83-92.
- Newell, A.J. 2006. Calcrete as a source of heterogeneity in Triassic fluvial sandstone aquifers (Otter Sandstone Formation, SW England). *Geological Society, London, Special Publications*, **263**, 119-127.
- Nilsen, H.M., Syversveen, A.R., Lie, K.-A., Tveranger, J. & Nordbotten, J.M. 2012. Impact of top-surface morphology on CO<sub>2</sub> storage capacity. *International Journal of Greenhouse Gas Control*, **11**, 221-235.
- Pharaoh, T.C., Morris, J., Long, C.B. & Ryan, P.D. 1996. The Tectonic Map of Britain, Ireland and adjacent areas. Sheet 1. 1:1 500 000 Scale. British Geological Survey and Geological Survey of Ireland.
- Pickup, G.E. & Hern, C.Y. 2002. The development of appropriate upscaling procedures. *Transport in Porous Media*, **46**, 119-138.
- Pickup, G.E., Jin, M., Olden, P., Mackay, E., Todd, A.C., Ford, J.R., Lawrence, D., Monaghan, A., Naylor, M., Haszeldine, R.S. & Smith, M. 2011. Geological storage of CO<sub>2</sub> : Site appraisal and modelling. *Energy Procedia*, **4**, 4762-4769.
- Pollard, J.E. 1981. A comparison between the Triassic trace fossils of Cheshire and South Germany. *Palaeontology*, **24**, 555-588.
- Schlumberger. 2013. ECLIPSE Reservoir Simulation Software, Technical Description.
- Shariatipour, S. M. 2013. Modelling of CO<sub>2</sub> Behaviour at the Interface between the Storage Formation and the Caprock. *Doctoral dissertation*, Heriot-Watt University.
- Shariatipour, S.M., Pickup, G.E. & Mackay, E.J. 2013. The Effect of Aquifer/Caprock Interface on Geological Storage of CO<sub>2</sub>. *Energy Procedia*, **63**, 5544-5555.
- Watson, R. 2014. Building the future. *Greenhouse Gases: Science and Technology*, **4**, 259-261.

Williams, J.D.O., Jin, M., Bentham, M., Pickup, G.E., Hannis, S.D. & Mackay, E.J. 2013. Modelling carbon dioxide storage within closed structures in the UK Bunter Sandstone Formation. *International Journal of Greenhouse Gas Control*, **18**, 38-50.

Willis, B.J. & Tang, H. 2010. Three-Dimensional Connectivity of Point-Bar Deposits. *Journal of Sedimentary Research*, **80**, 440-454.

Wright, V.P., Marriott, S.B. & Vanstone, S.D. 1991. A 'reg' palaeosol from the Lower Triassic of south Devon: stratigraphic and palaeoclimatic implications. *Geological Magazine*, **128**, 517-523.

## Figure Captions

**Fig. 1.** Schematic diagram showing two potential CO<sub>2</sub> storage mechanisms, (A) injection into an aquifer or hydrocarbon reservoir that is sealed by a caprock and has a large-scale structural closure, and (B) injection into a dipping open aquifer where much of the long-term storage results from dissolution of the CO<sub>2</sub> into the pore fluids or by residual trapping. Small-scale structural and stratigraphic traps ('bumps') along the migration path of the CO<sub>2</sub> plume may have a significant impact on storage as the buoyant plume migrates upwards along the interface (Goater et al. 2013).

**Fig. 2.** Map showing the distribution of the major Triassic basins in southern onshore Britain and adjacent offshore areas, WB (Wessex Basin), WG (Worcester Graben), CB (Cheshire Basin), EISB (East Irish Sea Basin), SNSB (Southern North Sea Basin). Mesozoic faults are shown as grey lines (Pharaoh et al. 1996) and the outcrop of the Sherwood Sandstone Group as black shading. The location of the study area is at Sidmouth in SW England.

**Fig. 3.** Schematic Triassic stratigraphy and lithofacies of southern Britain (after McKie and Williams (2009)). In general terms gravelly and sandy fluvial systems of the Sherwood Sandstone Group flowed to the north while the diachronous transgression of Mercia Mudstone Group playa lacustrine environments was toward the south. The stratigraphic position of this study at the contact between the Otter Sandstone Formation and the Mercia Mudstone Group is shown by a star. BSPB (Budleigh Salterton Pebble Beds), CPB (Chester Pebble Beds).

**Fig. 4.** (A) Map showing the location of the contact between the Sherwood Sandstone (Otter Sandstone Formation) and Mercia Mudstone groups in south Devon. Good exposures occur below High Peak to the west of Sidmouth and at Pennington Point just to the east. (B) Map showing the outcrop of the Otter Sandstone

Formation. The formation subcrops throughout much of the Wessex Basin to the east. Well data indicate a number of well-defined fault controlled depocentres. (C) Well correlation panel from outcrop into the subsurface. Section is flattened on the top of the Otter Sandstone Formation. The conglomeratic Budleigh Salterton Pebble Beds (BSPB) are shown by green shading. Overlying this formation, the Otter Sandstone Formation can be subdivided into a number of units, an anhydrite-rich unit at the base (A) overlain by a fluvial sheet sandstone (B) becoming mud-prone toward the top (C).

**Fig. 5.** (A) Large cliff exposure of the Otter Sandstone Formation and Mercia Mudstone Group contact below High Peak near Sidmouth, Devon (see Fig. 4 for location). Between the amalgamated sheet sandstones of the Otter Sandstone Formation and the mudstones of the Mercia Mudstone Group is a 15-20 m thick transition zone of interbedded sandstone and mudstone. The structure of this interval, which here was impossible to access, was investigated using a laser scanner (scan site indicated by star on Fig. 5A and Fig. 4A). The scanning produced a 3D digital outcrop model as well as orthorectified base maps (B) which could be used to accurately map sedimentary structure without the distortion of conventional photographs.

**Fig. 6.** Photograph showing the Pennington Point Member (PPM) at the western end of Sidmouth Beach. The base of the member is an erosion surface which cuts downward from left to right into the Chiselbury Member (CM) of the Otter Sandstone Formation (OSF). A sandstone body with flat top and concave-up base infills the scour; above this the sandstones tend to have flat bases and concave-down tops. The top of the Pennington Point Member is a rapid transition into the Sidmouth Mudstone Formation (SMF) of the Mercia Mudstone Group (MMG). White arrows highlight the base and top of the Pennington Point Member.

**Fig. 7.** Logged section of the transition zone (Pennington Point Member) between the Otter Sandstone Formation and the Mercia Mudstone Group showing the approximately equal proportions of sandstone and mudstone.

**Fig. 8.** (A) Sand-filled vertical burrow cross-cutting a mudstone bed and providing flow connectivity between two sandstone beds (pen lid is 30 mm long). (B) Mudstone bed with thin interbedded sandstones and sand-filled fluid escape structures (ruler scale is 20 mm across).

**Fig. 9.** (A) A simple porosity model of the outcrop created by the extrusion of the sandstone and mudstone units perpendicular to the digital outcrop model. While unrealistic this method has the advantage of speed,

and more importantly it maintains the spatial relationship of known mapped structures throughout the cube.

(B) Morphology of the CO<sub>2</sub> plume after 6 years of injection from an injector well located on the down dip (eastern) part of the static geological model (Fig. 8). Colour ramp shows percentage CO<sub>2</sub> saturation at 6 years from the start of injection.

**Fig. 10.** Cross-plot showing the porosity (%) versus the log of gas permeability (mD) for plug samples taken from outcrop of the Otter Sandstone Formation and neighbouring shallow boreholes. In the geological model the permeability parameters are mapped from porosity through the empirical correlation between porosity and permeability.

**Fig. 11.** Results of the Eclipse dynamic flow simulation shown on the vertical plane of laser-scanned digital outcrop model. Colour ramp shows percentage CO<sub>2</sub> saturation at 6 years from the start of injection. Red colours indicate a high gas saturation caused by pooling of the buoyant CO<sub>2</sub> below mudstone baffles.

**Fig. 12.** Plume migration at the end of the injection period (6 years) showing the effect of grid size on plume migration, (A) shows the base case model and (B) shows the coarse model. (C) Plot showing CO<sub>2</sub> dissolved in the water phase against time, Base case: one type of capillary pressure (Pc) was used, Case 2: two types of Pc curves were used, Case 3: three types of Pc curves were used, Case 4: four types of Pc curves were used.

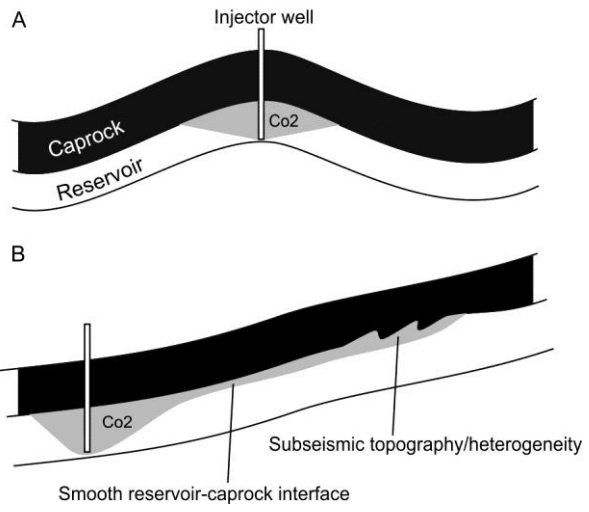


Fig.1

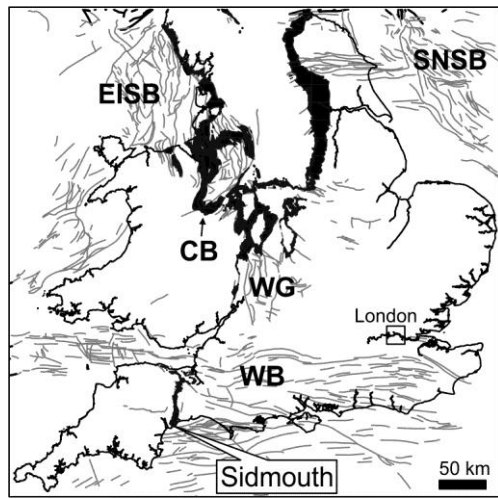


Fig.2

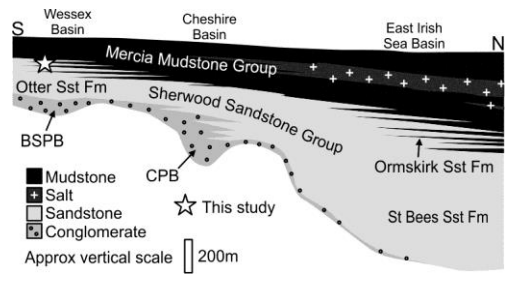


Fig.3

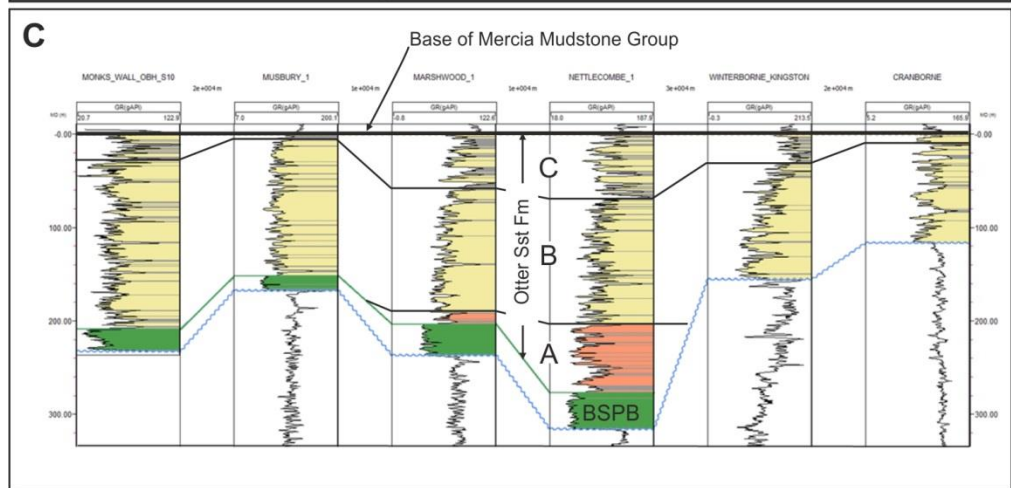
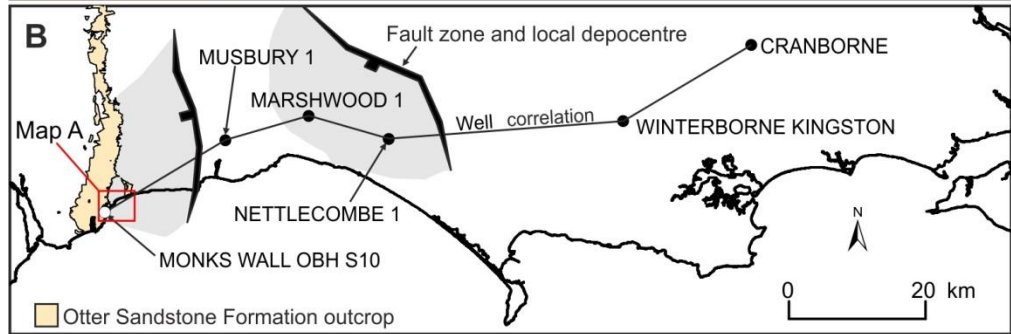
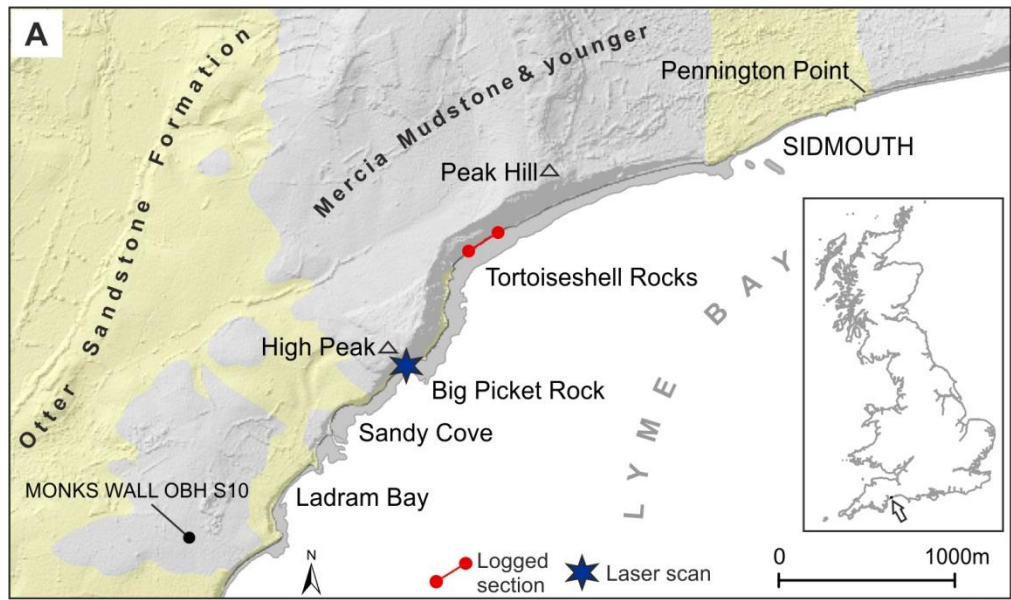


Fig.4

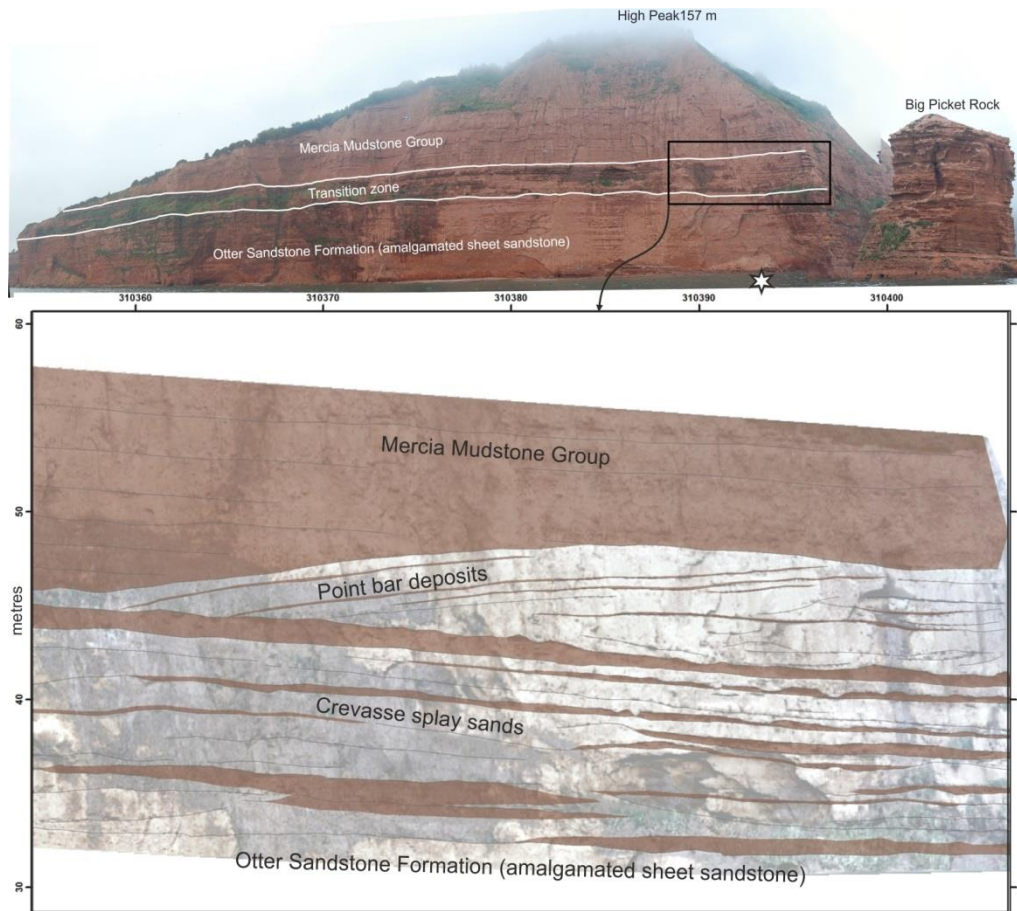


Fig.5



Fig.6

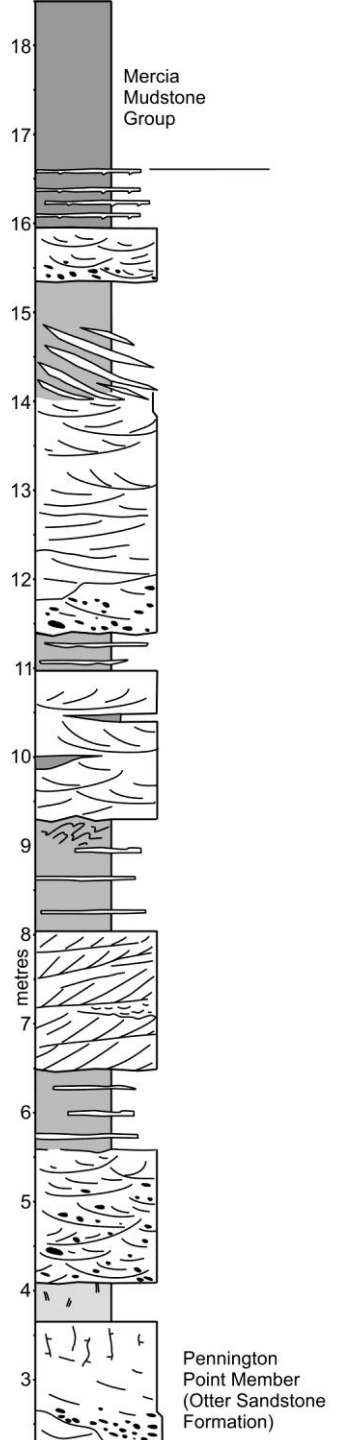


Fig.7



Fig.8

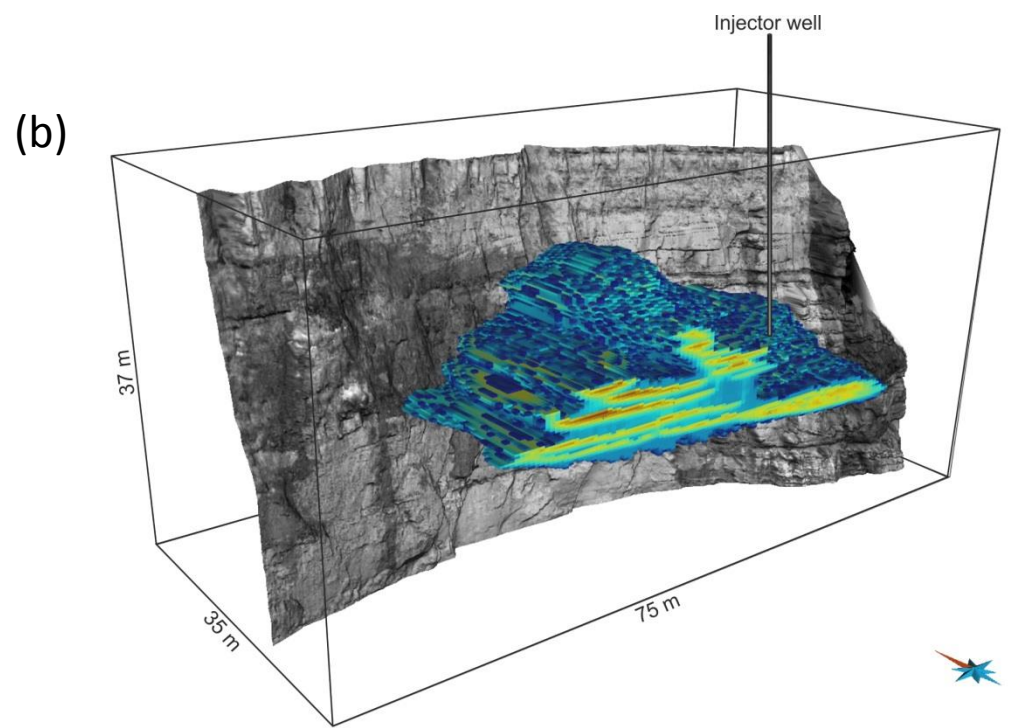
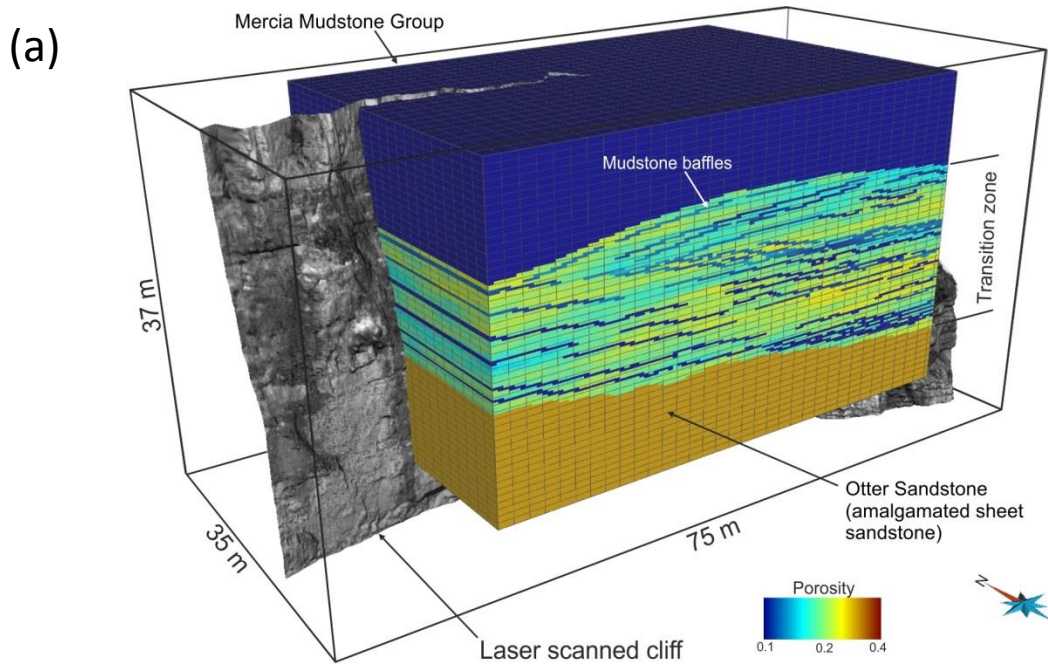


Fig.9

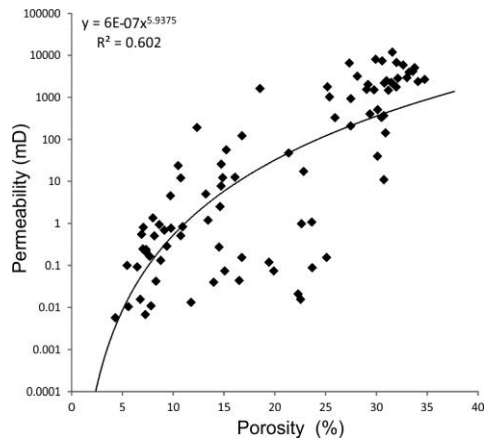


Fig.10

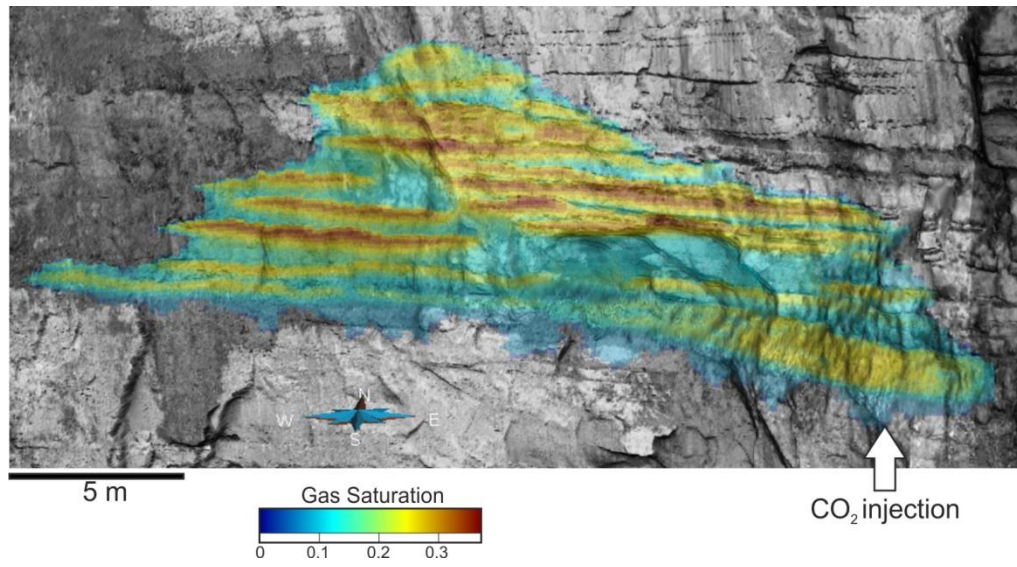


Fig.11

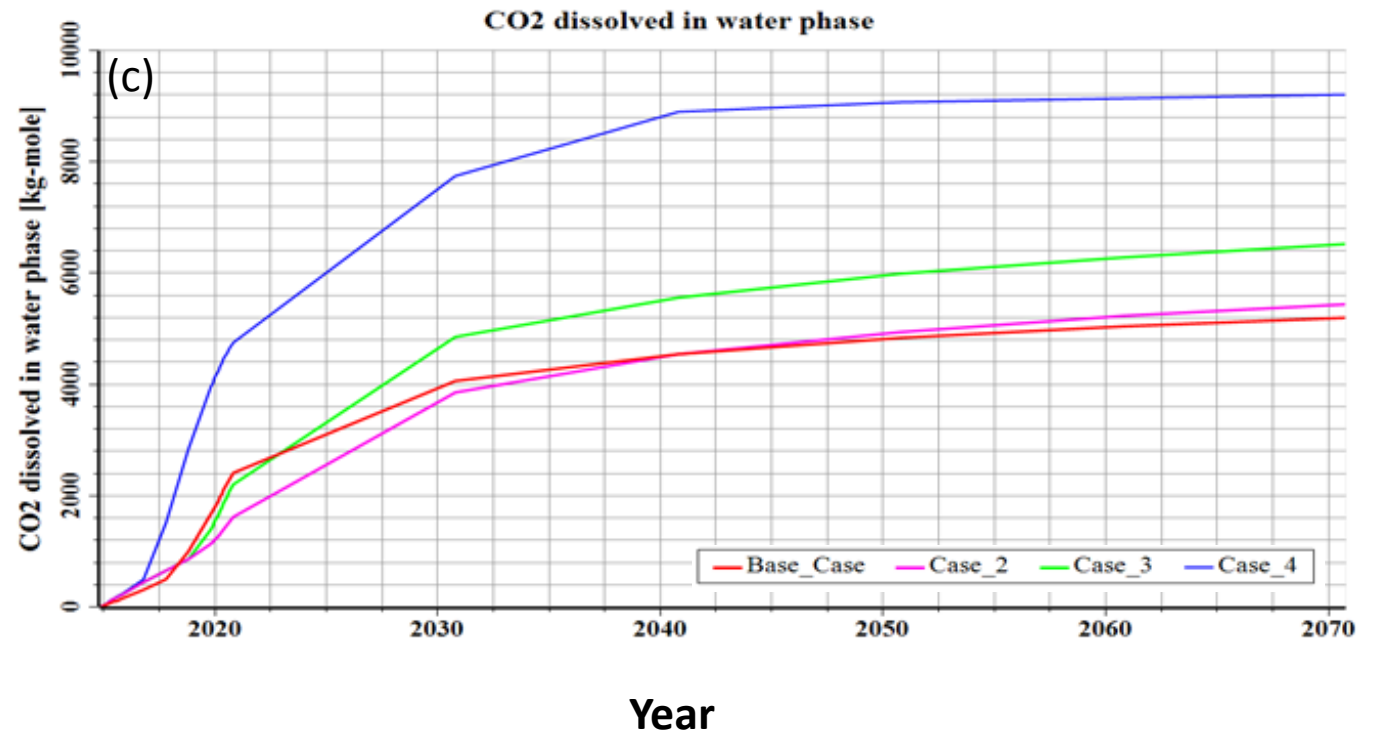
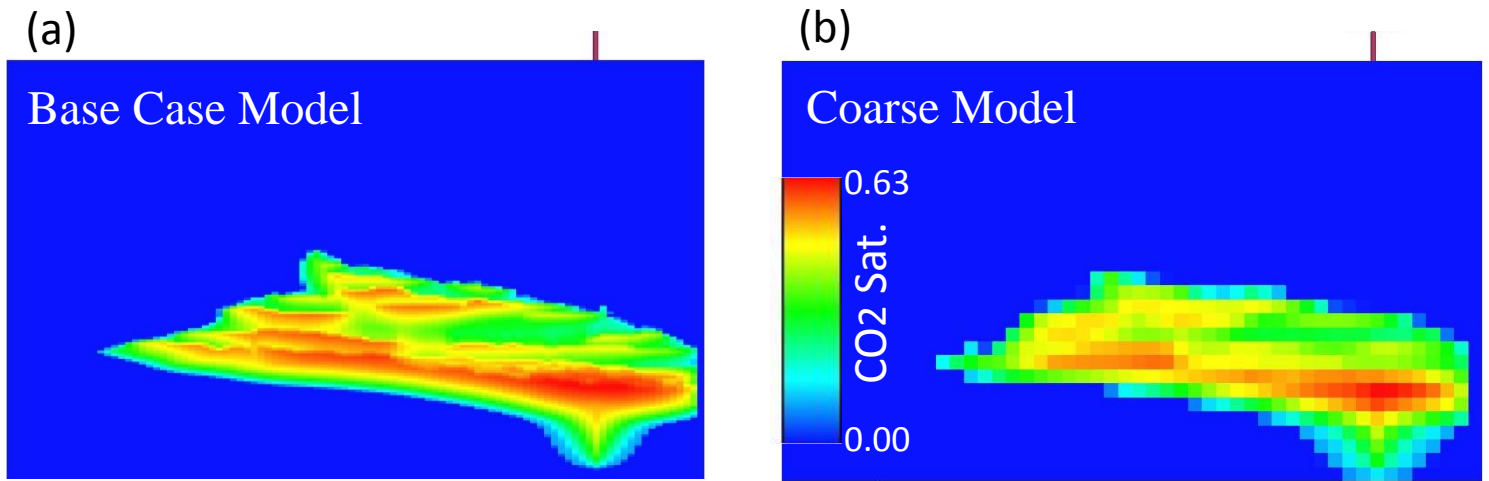


Fig.12